Anisotropic Behavior of X100 Pipeline Steel*

*J. Matthew Treinen[1,2], William E. Luecke[3], J. David McColskey[1], Philippe P. Darcis[1**], Yong-Yi Wang[4]*

[1]Materials Reliability Division
National Institute of
Standards and Technology
Boulder CO, USA

[2]Department of Civil
Engineering
University of Colorado
Boulder CO, USA

[3]Metallurgy Division,
National Institute of
Standards and Technology
Gaithersburg MD, USA

[4]Center for Reliable Energy
Systems
Dublin OH, USA

ABSTRACT

While steel is generally treated as being isotropic, tension and compression tests in the different pipe orientations for API X100 grade pipeline steel show that this is not the case. To better understand the anisotropy, tests in the longitudinal, transverse, short transverse and at 45 degrees in the L-T plane were performed. Three extensometers were oriented orthogonally to each other on the specimen, allowing for the calculation of the strain ratio, *R*. The results of these tests along with an analysis of the ratios are discussed.

KEY WORDS Anisotropy, Anisotropic Ratio, Pipeline, UOE, X100

INTRODUCTION

Fully understanding the material behavior of pipelines produces safer, more cost-effective pipelines. The use of complex material models can increase the accuracy of models of pipe behavior under buckling, wrinkling, reeling and other applied loads (Adeeb Zhou, and Horsley 2006, Wiskel et al. 2001, 2004, Martinez and Brown 2006, Liu and Wang 2006a,b). These analyses have emphasized modeling the kinematic shift in the yield surface in the transverse direction due to the expansion (E) stage of the UOE pipe forming process, where the pipe is first bent to a "U", then to an "O," welded together, and then (E)xpanded. During cold working of the steel during the UOE process, the grain orientations and dislocations are further modified (Dieter 1986). Also, complex thermo-mechanically controlled (TMCP) forming processes introduce textures or preferred orientations within the steel. Both of these are known to affect the anisotropic behavior of the steel.

One method to quantify the anisotropic behavior is to use the Lankford strain ratio, or *R*-value (Dieter 1986). It is beneficial to understand this strain behavior, particularly under large deformations, as a supplement to anisotropic yield stress determination. In this study of the anisotropy of API X100 pipeline steel, three extensometers were used to measure the orthogonal strains in both tension and compression specimens with different orientations relative to the pipe. From the extensometers it was possible to calculate the anisotropy ratios.

TEST PROCEDURE

The X100 linepipe used in this study had a 914 mm diameter and a 14.3 mm wall thickness; the chemical composition is given in Table 1.

Table 1. X100 Chemical Composition

C	Si	Mn	P	S	Nb	V	Ti	Al
0.058	0.223	1.960	0.007	0.002	0.045	0.000	0.014	0.003
Ni	Cu	Cr	Mo	B	N	O	Ceq	Pcm
0.300	0.210	0.020	0.180	0.000	0.003	0.002	0.460	0.190

Tensile tests were performed in three different directions relative to the pipe orientation, as shown in Figure 1. Unfortunately due to the small wall thickness of the pipe, it is not possible to extract the tensile properties through the thickness using standard specimens. To supplement the tensile tests, compression tests were also performed using specimens in the same three directions as the tensile tests and also in the short-transverse direction (ST). The tensile specimens had a 6.35 mm diameter and 31.8 mm uniform gage length with 12.7 mm diameter threaded ends. Testing was performed with a 100 kN servo-hydraulic test frame and a constant strain rate of 1.0×10^{-4} s^{-1}. The diameter of the compression specimens was 6.35 mm and length of 10 mm, except specimens CT-1 which had a length of 12.7 mm. They were tested on a 50 kN servo-hydraulic test machine with loading rams fabricated from maraging steel. Teflon tape lubricated the compression specimen ends to minimize barreling due to friction.
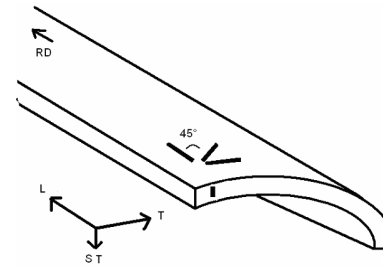

Figure 1. Schematic of test specimen orientation

To better understand the ovalization of the specimen during testing, two diametral extensometers were attached to the specimen. They were oriented so that one measured the contraction in the short-transverse (ST) direction and the other measured the contraction perpendicular to the ST direction. For example, for the test in the transverse direction, one extensometer measured the diametral strain in the short transverse while the second extensometer measured the strain in the longitudinal direction. Figure 2 shows the actual test setup used for the tensile tests; the same orientation was used for the compression tests. The axial extensometer was an ASTM Class B-2 extensometer with a 25.4 mm gage length. The two diametral extensometers were custom built.
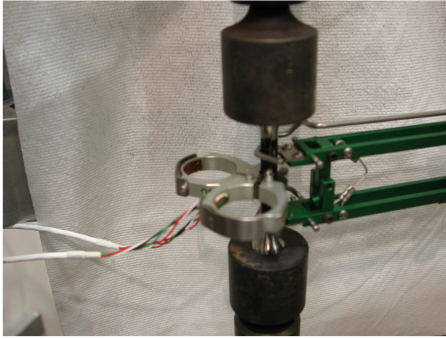

Figure 2. Test setup for tensile testing.

One limitation of the diametral extensometers is that their jaws are 4.25 mm high, as shown in Figure 2. Therefore, the extensometer measures only the largest diameter over that height; it is unable to capture localized necking or barreling. Affixing knife edges to the extensometers would provide a more localized strain measurement, but attaching the gage to the specimen and ensuring that it does not move would be more difficult. Nonetheless, it is most important to capture the diametral strains up to the tensile strength, which the extensometers can adequately capture, since no localized necking is present.

RESULTS

Stress-Strain Behavior

Figure 3–6 show the resulting true stress-true strain curves up to the tensile strength in the four directions: longitudinal (L), Transverse (T), at 45 degrees in the LT plane (LT-45) and short-transverse (ST), respectively.
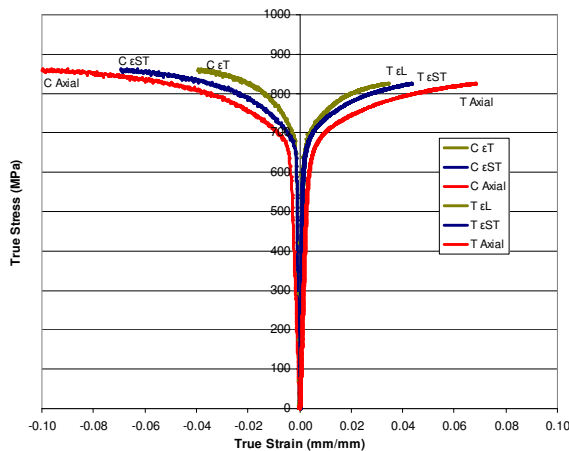
While the diametral strains in the tension tests are actually negative, they are plotted as being positive to more easily compare them to the axial strain. In the same regard, the positive diametral strains in the compression test are plotted negative in the figures. The compression tests were ended at approximately 10 % axial strain to prevent the platens from touching the diametral extensometers. Although two
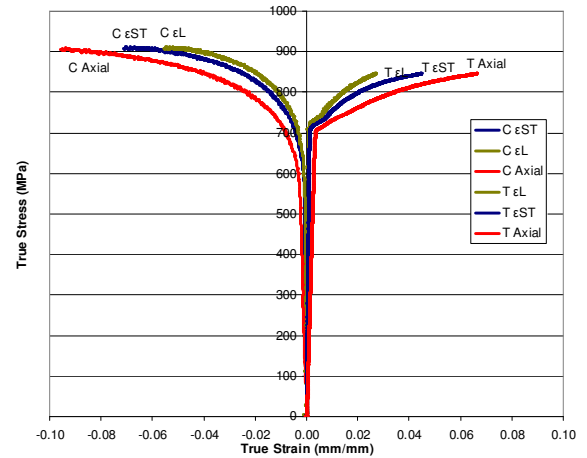

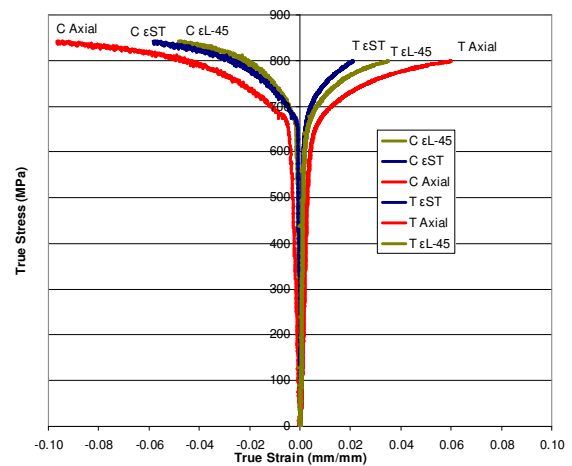Figure 4. True stress-strain behavior (Transverse).

Figure 5. True stress-strain behavior (45 degree in LT Plane).

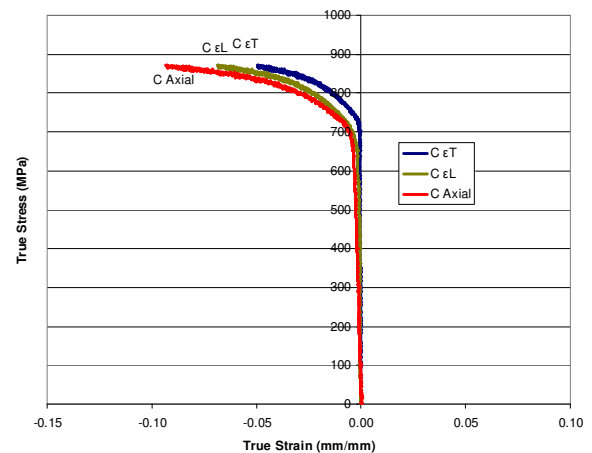Figure 3. True stress-strain behavior (Longitudinal).

Figure 6. True stress-strain behavior (Short Transverse).

specimens in each direction were tested, the results for only one test are plotted, since the stress-strain behaviors were similar.

Strain Ratios

To better understand the differences between the diametral strains, it was possible to plot the plastic strain ratio, or Lankford R-value, for the tests defined by the following (Dieter 1986):

$$R = \varepsilon_w / \varepsilon_t \qquad (1)$$

where ε_w is the strain in the width direction of the sheet and ε_t is the strain in the thickness direction of the sheet. Because of the different orientations of the tests, the definitions of ε_w and ε_t change. The test-specific definition of R is shown in each of the figures. Figures 7-10 plot the R values as a function of true stress for the four different test orientations.
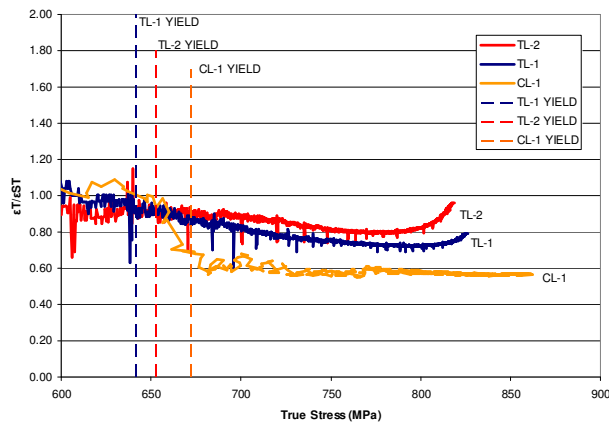

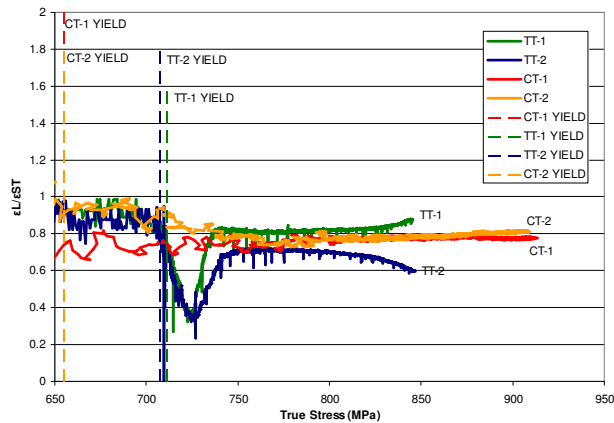Figure 7. Anisotropic ratios from longitudinal tests.

Figure 8. Anisotropic ratios from transverse tests.
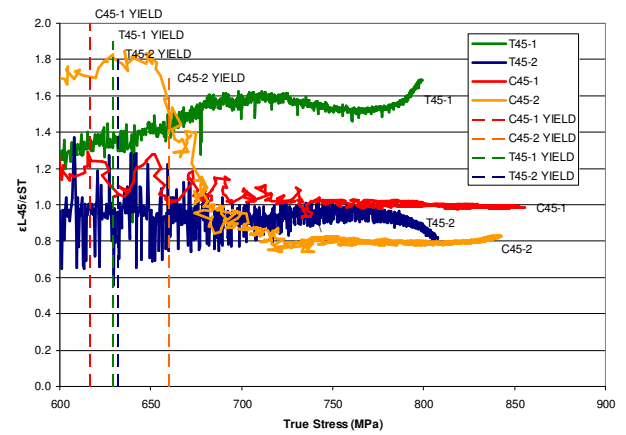

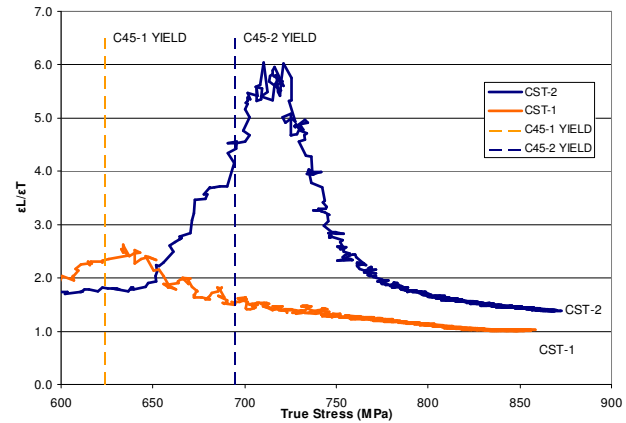Figure 9. Anisotropic ratios for LT45 tests.

Figure 10. Anisotropic ratios from short transverse tests.

DISCUSSION

From the stress-strain curves, it is possible to calculate the yield stresses from the different tests; Table 2 summarizes the results. The YS 0.002 uses the 0.2 % offset method for finding the yield stress, the other results are the stresses at the total strains, 0.5 %, 1 % and 2 %. The repeatability of results of the tensile tests was high, but the repeatability in the compression tests was lower.

Table 2. Summary of yield stresses for the tests (MPa).

Test	YS 0.002	YS 0.005	YS 0.01	YS 0.02
CL-1	677	671	716	772
CL-2	-	-	-	-
CT-1	656	655	729	802
CT-2	658	655	703	809
C45-1	631	617	700	769
C45-2	676	660	689	752
CST-1	637	624	707	768
CST-2	704	695	740	790
TL1	645	642	695	730
TL2	655	653	696	729
TT-1	711	711	724	744
TT-2	707	707	724	747
T45-1	636	629	680	716
T45-2	639	632	686	720

Also, unlike the gradually sloping result at yield in the stress-strain curves for the other tests shown, the knee in the tensile tests in the transverse direction is sharp. Cold working of the steel in the transverse direction as the pipe is expanded during the UOE formation process produces this sharp knee (Liu and Wang 2007b). The absence of the knee in the short-transverse compression tests is due to the Bauschinger effect (Liu and Wang 2007b).

To further explore this effect of the cold expansion in the transverse direction, Figure 11 shows a plot of the axial stress-strain response shifted from zero strain and plotted against the longitudinal stress-strain curve. By shifting the transverse stress-strain curve it is possible to predict the plastic strain introduced into the pipe in the transverse direction during the expansion process as being 0.6 %. This plastic strain falls in the range of 0-5 % strain that the pipe may experience during forming (Wiskel 2001).
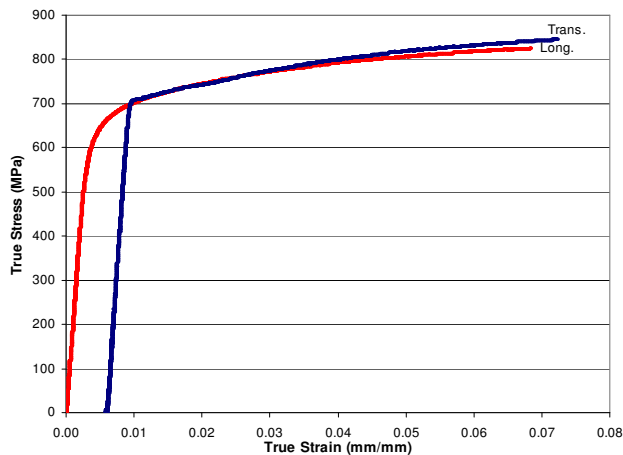

Figure 11. Shift of Transverse stress-strain curve to predict induced plastic strain.

The strain level at which to measure the anisotropy ratios is debated among researchers. Figures 7, 8, 9, and 10 demonstrate that the strain ratios, R, are not constant with strain. Researchers who focus on sheet forming and drawing generally measure the strain ratio just below the ultimate strength, since necking and thus material failure are critical in the forming processes. However, for studies of the effect of metallurgical texture, it is often more beneficial to look at the strain ratio at zero strain. Extrapolation of an empirical $R(\varepsilon)$ expression back to zero strain allows comparison of the strain ratios of the undeformed microstructure and enables analysis of the effect of metallographic texture (Truszkowski 2001). While it would be beneficial to expand this current study to compare the strain ratios at zero strain with the microstructure and texture of the steel, the following discussion will focus on the ratios during plasticity, which is more pertinent to the large-strain performance and strain-based design of pipelines.

One method to analyze the accuracy of the strain ratios plotted in Figures 7−10 is to measure the two diameters of the deformed specimens and calculate the strain ratios from these measurements. For the compression tests, this was done over the length of the specimen and the values averaged, while for the tension specimens, which had been tested to failure, the measurements were made on each half of the specimen at points outside of the necked region. Table 3 compares these ratios to the average ratios from Figures 7−10, where "R meas" is calculated from the diameter measurements after the test, and "R ext" is calculated from the extensometers.

The R values of tests CT-1, CST-1, TL-1, TT-1, and T45-2 calculated from both methods are similar, which demonstrates that the extensometers accurately recorded the strain ratio. The larger discrepancies in the other tests highlight the difficulty in accurately measuring the diametral strains by use of the extensometers. The following discussion considers only these five tests

The plastic strain ratio in the transverse tension tests (TT-1 and TT-2) dips sharply just after yield, Figure 8. A corresponding dip is absent in the compression tests. Furthermore the dip is present only in the transverse and not in the longitudinal or short-transverse tests. The source of this dip is unknown.

Table 3 comparison of R value measuring technique.

Test	R meas	R ext	Diff.
CL-1	0.67	0.55	-17.6%
Cl-2	0.87	-	-
CT-1	0.74	0.74	0.0%
CT-2	0.87	0.77	-11.4%
C45-1	1.08	0.97	-10.0%
C45-2	1.02	0.78	-23.6%
CST-1	1.17	1.13	-3.1%
CST-2	1.25	1.81	45.0%
TL1	0.74	0.73	-2.0%
TL2	0.72	0.81	11.8%
TT-1	0.78	0.77	-2.0%
TT-2	0.82	0.63	-23.1%
T45-1	1.12	1.49	33.5%
T45-2	1.14	1.12	-1.6%

Although the strain ratio is often taken to be constant (Honeycombe 1984), it changes with strain in this X100 steel. A large region of constant strain ratio is present at large strains but a large region of varying strain ratio exists at smaller strains. Truszkowski (2001) clarifies that for polycrystalline materials such as steel, an initial region of instability occurs due to changing slip systems, which leads to twinning or shear banding, during which the ratio becomes constant. Furthermore, as the strain increases, the ratio gradually decreases rather than remaining constant. Both of these trends occurred in the five valid tests.

To illustrate the anisotropic behavior, the strain ratios can be plotted as polar vectors relative to the rolling direction (Truszkowski 2001), as shown in Figure 12. From the tests, it is possible to plot this pole figure in the LT plane only. However, with additional tests at angles in the L-ST and T-ST directions, further understanding of the anisotropy through the thickness could be gained. Tests at angles other than 45° in each of the planes would also further clarify the pole diagrams. In Figure 12, the ratios for all twelve of the tests are plotted as points (diamonds) to show the scatter in the R values. The ratios calculated from tests TL-1, TT-1, and T45-2, shown to be the most accurate, are the ends of the polar vectors.
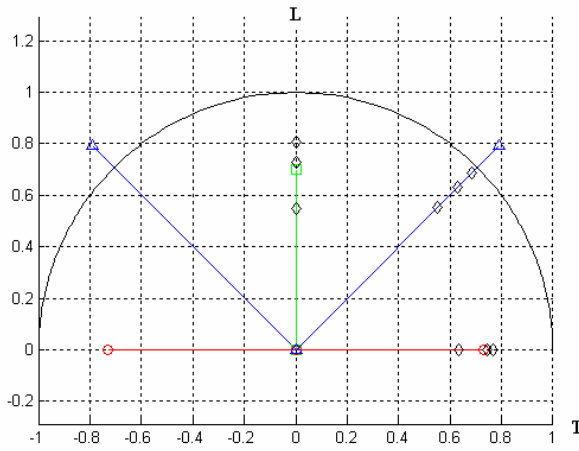
Figure 12. Pole figure for LT plane.

The strain ratio in the transverse direction is just slightly higher than in the rolling direction; both are less than unity. However, the strain ratio is just slightly higher than one at 45˚. This suggests that in the longitudinal and transverse tests the short-transverse strain is higher compared to the perpendicular diametral strain; yet, at 45˚, the strain is lower in the short transverse direction. Although this behavior is unexpected, measurements of the diameter of all four of the 45˚ specimens verified that it is correct. Further analysis of the microstructure and texture may clarify this behavior.

Post Failure Behavior

Because of the extensometer thickness, it is not possible to accurately capture the area reduction during necking by use of the extensometers. However understand the behavior after ultimate strength, it was possible to measure the final cross-sectional area after failure of the tensile specimens and find the two radii of the deformed elliptical cross section. The strain ratio at failure, R_f , was calculated from the minimum, r_{min}, and maximum, r_{max}, radii of the specimen fracture surface. Table 4 shows the results, along with the average strain ratios measured before necking using the diametral extensometers.

Table 4. Comparison of radii at failure to R-values.

Tension	r_{max} (mm)	r_{min} (mm)	R_f	Average Strain Ratio
TL-1	1.37	0.67	0.54	0.73
TT-1	1.43	0.84	0.60	0.77
T45-2	0.94	0.81	1.12	1.12

The strain ratio calculated from the radii of the fracture surface of specimen T45-2 was nearly equal to the average strain ratio from the figures above. The diametral deformation remained constant between the tensile strength and fracture in LT-45 direction. However, in the longitudinal and transverse tests, TL-1 and TT-1 the ratios are quite different; more ovalization occured after the tensile strength in the neck.

CONCLUSIONS

Through tensile and compression testing using both an axial extensometer and two diametral extensometers, it was possible to further understand the anisotropic behavior of X100 pipeline steel. It was possible to calculate the yield strengths in the different material directions and verify that the sharp knee in the transverse direction is due to the cold expansion during the UOE process. Further, the longitudinal and transverse strain ratios, R, are below unity, 0.73-0.77, while at 45 degrees in the LT plane the ratio, 1.12, is just above unity. The strain ratio in the short transverse direction in compression was 1.13. Further testing in the T-ST and L-ST planes are necessary to completely describe the anisotropy. Also, further analysis of the effects of microstructure and texture would enhance the anisotropy analysis.

REFERENCES

Adeeeb S, Zhou J, Horsely D.(2006) "Investigating the Effect of UOE Forming Process on the Buckling of Line Pipes Using Finite Element Modeling" *Proc. of IPC 2006*, Calgary. IPC2006-10175.

Dieter GE. (1986) *Mechanical Metallurgy*, 3nd Ed. New York: McGraw-Hill.

Honeycombe RWK. (1984) *The Plastic Deformation of Metals*, 2nd Ed. London: Edward Arnold.

Liu M, Wang YY. (2007a) "Advanced Modeling of Plasticity of Linepipe Steels with Aniostropic Texture and Complex Loading History" *Proc. of the 17th ISOPE*, Lisbon, pp 3093-3100.

Liu M, Wang YY. (2007b) "Modeling of Anisotropy of TMCP and UOE Linepipes" *Intl J of Offshore and Polar Eng*, Vol 14, No 4, pp 288-293.

Martinez M, Brown G. (2005) "Evolution of Pipe Properties During Reel-lay Process: Experimental Characterization and Finite Element Modeling" *Proc. of OMAE 2005*, Halkidiki, Greece, Vol 3, pp 419-430.

Truszkowski W. (2001) *The Plastic Anisotropy in Single Crystals and Polycrystalline Metals* Dordrecht: Kluwer.

Wiskel JB, Owens C, Rieder M, Thiessen R, Henein H (2001) "Modeling the forming of microalloyed steel pipe" *Proc. of the Symposium on Innovative Technologies for Steel and other Materials*, MetSoc of CIM, Montreal, pp 369-382.

Wiskel JB, Rieder M, Henein H.(2004) "Kinematic Behaviour of Microalloyed Steels Under Complex Forming Conditions" *Canadian Metallurgical Quarterly*, Vol 43 No 1, pp 125-136.